ICES Journal of Marine Science, 2023, **0**, 1–14
DOI: 10.1093/icesjms/fsad137
Original Article

Modelling and *in situ* observation of broadband acoustic scattering from the Silver cyprinid (*Rastrineobola argentea)* in Lake Victoria, East Africa

Yang Yang [1,*], Sven Gastauer [2,3], Roland Proud [1], Richard Mangeni-Sande [1,4], Inigo Everson [1,5], Robert J Kayanda [6], and Andrew S Brierley [1]

[1]Pelagic Ecology Research Group, School of Biology, Scottish Oceans Institute, Gatty Marine Laboratory, University of St Andrews, Fife KY16 8LB, UK
[2]Integrative Oceanography Division, Scripps Institution of Oceanography, La Jolla, CA 92093, USA
[3]Thünen Institute of Sea Fisheries, 27572 Bremerhaven, Germany
[4]National Fisheries Resources Research Institute, PO Box 343, Jinja, Uganda
[5]School of Environmental Sciences, University of East Anglia, Norwich Research Park, Norwich NR4 7TJ, UK
[6]Lake Victoria Fisheries Organization, PO Box 1625, Jinja, Uganda

[*] *Corresponding author:tel: +44 (0)7529 91 0754;* e-mail: yyy1@st-andrews.ac.uk.

Lake Victoria is the second-largest freshwater lake in the world, and fish from the lake are a vital food resource for millions of people living around it. The silver cyprinid (*Rastrineobola argentea),* a small schooling pelagic species known in Tanzania as "dagaa" contributes ca. 55% to the total annual catch (ca. 0.51 million tonnes (MT) in 2014). The acoustic target strength (TS, dB re 1 m^2) of dagaa, a key factor for biomass estimation, is however not well described, and is a major source of uncertainty in biomass estimation. In this study, we developed a Kirchhoff-ray mode (KRM) model to predict the TS of dagaa at standard fisheries survey frequencies. The model was based on the morphology of the body and the dual-chambered swimbladder, as obtained from X-ray images of fish ranging in total length (TL) between 2.8 and 5.4 cm. The results suggested that the swimbladder (which comprises 2.6 to 8.2% of body volume) accounts for ca. 65 to 90% of the total backscattering at 120 kHz. The predicted TS was highly dependent on tilt angle, varying by 14.0 dB at 120 kHz across the tilt range 65–115° (where 0° is head up and 180° is tail up), and TS variability with tilt generally increased with increasing frequency. The tilt angle of acoustically tracked individual fish indicated a distribution of tilt angles with a mean and s.d. of 93.5 and 15.1°. Our model suggested a new tilt-averaged TS–TL relationship for dagaa [$TS_{120\ kHz} = 19.49\log(TL) - 70.3$], which leads to a TS 1.5 dB higher than the value in the relationship presently used to estimate stock biomass. The new relationship will lead to a substantial reduction (by ca. 30%) in estimated biomass. The discrepancies between the mean relative frequency response of the *in situ* measurements of backscatter from dagaa and the KRM model predictions were in the range of -2.9–3.1 dB at frequencies from 45 to 250 kHz. The KRM modelling and *in situ* broadband measurements of dagaa will be beneficial for acoustic identification and behavioural studies of dagaa, and will enable improved biomass assessment, thereby underpinning sustainable long-term management.

Keywords: frequency response, KRM, physostomes, swimbladder, target strength, X-ray.

Introduction

Lake Victoria is the second-largest freshwater lake in the world. Fish and fishing provide important sources of food and employment for local communities. Long-term sustainable management of Lake Victoria's fisheries resources is therefore vital for food security and economic well-being, as well as for preserving ecosystem functions. The indigenous silver cyprinid (*Rastrineobola argentea*, known locally in Tanzania as "dagaa") is one of the most important species in the lake ecologically and economically. Dagaa make up about 55% of the total annual catch from the lake (dagaa catch in 2014 was ca. 0.51 million tonnes (MT)), with a market value of about USD 135 million (LVFO, 2016). According to acoustic estimates, dagaa make up around 27–44% of the lake's total fish biomass (LVFO, 2012; Tumwebaze, 2018). There are, however, considerable uncertainties in stock estimates due to a limited understanding of the acoustic scattering properties of dagaa. This impacts species identification and the scaling of acoustic backscattering intensity to biomass.

Acoustic estimation of fish biomass in Lake Victoria began in the late 1990s, and annual or bi-annual surveys have been run ever since. Target Strength (TS, dB re 1 m^2) is the key factor for converting measured acoustic backscatter into biomass. TS is dependent on a variety of factors (including target size, tilt angle, material properties, and acoustic frequency) with some stochasticity. TS should ideally be well described as a foundation for any acoustic-based biomass estimate, since small changes can have large influences on results (Demer and Conti, 2005), and with uncertainties in TS propagating to uncertainties in biomass estimation (Gastauer *et al.*, 2017). The TS of dagaa at conventional acoustic survey frequencies (70, 120, and 200 kHz in Lake Victoria) is not well described, and the broadband scattering spectrum of the species has not yet been studied. Before 2003, dagaa biomass was determined using the TS–total length (TL) relationship ($TS_{120\ kHz} = 20log_{10}(TL(cm)) - 71.2$) derived for North Sea herring (*Clupea harengus*), a species that is only superficially similar to dagaa (Foote *et al.*, 1986). Presently, the

Received: 11 June 2023; **Revised:** 10 August 2023; **Accepted:** 14 August 2023

standard stock biomass estimate is using the TS–TL relationship ($TS_{120\ kHz} = 20log_{10}(TL(cm)) - 72.2$) adopted from Tumwebaze *et al.* (2003), which was derived from *in situ* cage measurements of dagaa at 120 kHz; this relationship does not consider tilt angle variation. It is well known that changes in tilt angle can have major impacts on fish TS. For example, modelling suggests that the TS of Pacific hake (*Merluccius productus*) can change by up to 26 dB at 120 kHz over the quite narrow range of tilt 80–100° (where 90° is dorsal-aspect incidence) (Henderson *et al.*, 2008): tilt variability has the potential, therefore, to introduce huge uncertainty and bias to biomass estimation (a change of 3 dB translates to a twofold change in the linear domain).

Scattering properties of organisms can be obtained by direct (i.e. *in-situ* and *ex-situ* measurement) or indirect (i.e. modelling) methods. The direct methods might suffer from interference noise from other sources (e.g. vessel and ship-borne acoustic Doppler current profiler (SADCP)) and fish mortality during handling and operation. Model simulations are more flexible and enable the analysis of variation in sound scattering by fish as a function of incident angle, size, and a range of other factors, including acoustic impedance and different body shapes and internal structures. The most commonly used scattering models can be divided into three main categories: (1) exact analytical models, which are used mainly to simulate the scattering of simple geometric shapes such as spheres and bent cylinders; (2) quasi-exact numerical models, which are used to simulate the scattering of arbitrary shapes and materials, considering diffraction, but which are computationally expensive [e.g. FEM (finite element method), BEM (boundary element model)]; and (3) approximate analytical models, which can simulate the scattering of complex shapes at high frequencies, and for which calculation is comparatively simple and which are presently the most widely used [e.g. KA (Kirchhoff approximation), KRM (Kirchhoff-ray mode), DCM (deformed cylinder model), DWBA (distorted wave Born approximation)]. To date, a large number of models have been developed for predicting the acoustic backscatter of a variety of species of fish (e.g. Jech *et al.*, 2015).

The KRM model was initially conceived by Clay and Horne (1992) to describe the backscattering of Atlantic cod (*Gadus morhua*) and has been further developed and applied to many fish species (Henderson *et al.*, 2008; Fassler, 2010; Antona, 2016; Gastauer *et al.*, 2016; Manik, 2016). The KRM model calculates backscatter for an entire fish as the summation of backscatter from a set of gas-filled or fluid-filled cylinders that together represent the entire fish. It accounts for reflection coefficients from front and back interfaces between cylinders and requires only a low computing effort. The swimbladder can account for up to 95% of the total backscatter at 38 kHz from swimbladdered fish (Foote, 1980). Dagaa have a dual-chambered swimbladder and are physostomous: they have a pneumatic duct (on the posterior chamber) connected to the oesophagus and might be able to gulp air through the duct to inflate the bladder (Figure 1). By X-ray scanning fish dorsally and laterally, the 3D morphometry of the swimbladder and fish body can be built separately and used as inputs to the KRM model.

Another key factor in biomass assessment is species identification: detected acoustic energy needs to be partitioned across various species/groups in the survey area (Korneliussen, 2018). Traditional methods of echo-energy partitioning include visual scrutinization and the allocation of acoustic energy based on the species composition of net catch samples (McClatchie *et al.*, 2000). For dagaa in Lake Victoria, the standard partition approach has been a depth-based rule, with all echo energy returning from the top third of the water column (after removal of single targets believed to be Nile perch (*Lates niloticus*)) being designated to dagaa (Taabu-Munyaho *et al.*, 2014). This rule is based on the assumptions that dagaa are the only schooling species to occur in the top third of the water column and that no dagaa occur below this depth; this is now known to be incorrect (Proud *et al.*, 2020). Proud *et al.* (2020) developed an automated acoustic classification method for dagaa that used a random forest approach to identify dagaa schools in echograms based on school morphology, but that method used only 120 kHz data. Broadband measurements can potentially provide more information when classifying detected targets than single or multifrequency data since they can be used to characterize the frequency response of targets over a wide frequency band (Stanton *et al.*, 2010). Jech *et al.* (2017) reported that the *in situ* broadband measurements of butterfish (*Peprilus triacanthus*) corresponded well with KRM model simulations and recommended the incorporation of broadband methods into the acoustic classification process. Benoit-Bird and Waluk (2020) showed that classification of acoustic targets as hake (*M. productus*), anchovy (*Engraulis mordax*), and krill (*Euphausiia pacific*) based on broadband measurements outperformed classification based on simulated multifrequency data. Presently, there is a paucity of information on the acoustic scattering properties of dagaa; consequently, there is a vital need to establish an approach for tackling the related challenges. To the best of our knowledge, broadband echosounder observations have not yet been used to classify fish echoes collected in Lake Victoria. Given that previous methods of dagaa classification were based on single-frequency observations, the development of broadband classification methods will likely provide substantial improvements to species identification and, therefore, stock assessment.

The objectives of this study were to: (1) develop an approximate KRM for dagaa based on X-ray imagery (of 16 fish) to simulate the backscatter over a wide range of sizes, tilt angles, and acoustic frequencies; and (2) compare the model simulation of dagaa with *in situ* broadband measurements to test the utility of the approach in performing dagaa species classification. The results could be used to improve dagaa species classification and biomass estimation. This is an important step to progress towards ecosystem-based fisheries management (EBFM) in Lake Victoria.

Materials and methods

Dagaa were sampled acoustically and by trawl from the *R.V. Victoria Explorer* (length 16.5 m; width 5.5 m) during a voyage in the north of Lake Victoria in Uganda (Figure 2) between 28th February and 3rd March 2022. X-rays were used to obtain 3D morphological of the entire bodies and swimbladders of dagaa (laterally and dorsally). A KRM scattering model was developed based on this 3D shape information. Tilt-averaged TS–TL relationships were developed based on the KRM approximation at frequencies used commonly for fisheries stock assessment (70, 120, and 200 kHz), and KRM-modelled continuous spectra were compared with *in-situ* broadband observations of dagaa (over the range of 45–250 kHz) identified by trawl sampling.

Figure 1. A dissected dagaa showing the structure of its dual-chambered swimbladder (red dotted line).

Trawl sampling

Dagaa were sampled using a pelagic trawl net with a cod end mesh size of 25.6 mm. Twelve trawls were conducted, following standard Lake Victoria Fisheries Organization (LVFO) protocols (LVFO, 2019). Trawls were carried out at various depths (the headline depth ranged from 8.6 to 41.3 m) to sample dagaa across a broad depth range (Proud *et al.*, 2020). The depth of the net was monitored in real-time using a Simrad PX multisensor (Mk. 2 catch monitoring sensor) attached to the headline, and the maximum depth of the foot line was determined *post-hoc* from a SCUBA depth gauge attached to the foot line. The real-time depth measurements were recorded using a Simrad SR15 hydrophone unit. Each trawl was about 15 min duration, and the vessel speed was 2 to 3 knots. After fishing, the net trajectory was reconstructed over the echogram with reference to net depth (from the net monitor) and warp length (that, with speed, gave the time/distance of the net behind the vessel). Regions where dagaa dominated by mass in the trawl catch were combined with acoustic observation for further analysis.

Due to the small size and mass of individual dagaa, fish bodies and swimbladders can easily be damaged during trawl recovery. To identify intact fish for X-ray, subsamples were taken from the codend and placed in a bucket filled with lake water, observed for 5 min to determine the status of individuals, and only live fish were preserved for further use. We assumed that sinking dagaa had ruptured swimbladders, floating dagaa had distended swimbladders, and that swimming dagaa had swimbladders close to their natural state, hence that swimming fish were intact. The sinking, swimming, and floating dagaa were separated, stored in a refrigerator, and taken to a local hospital (in Jinja, Uganda) for X-ray measurements on the same day that they were caught. Since dagaa are small [body mass (M) around 1 g], it is not easy to weigh them onboard or to get accurate mass results from frozen samples. Therefore, we used an empirical length-mass relationship (LVFO, 2012) to obtain mass:

$$M = 0.0231TL^{2.482} \quad (1)$$

Length distribution and species composition were determined from trawl samples. The catch composition and size distribution were determined for the entire trawl sample when the catch was <200 individual fish and for a random subsample of 200 fish when the catch number was >200.

In-situ broadband measurements

Acoustic data were collected with a Simrad EK80 echosounder (3 wide band transceivers or WBTs) operating in broadband mode (FM, frequency modulated) across a bandwidth of 45–250 kHz using transducers with central frequencies of 70, 120, and 200 kHz (Table 1). The WBTs

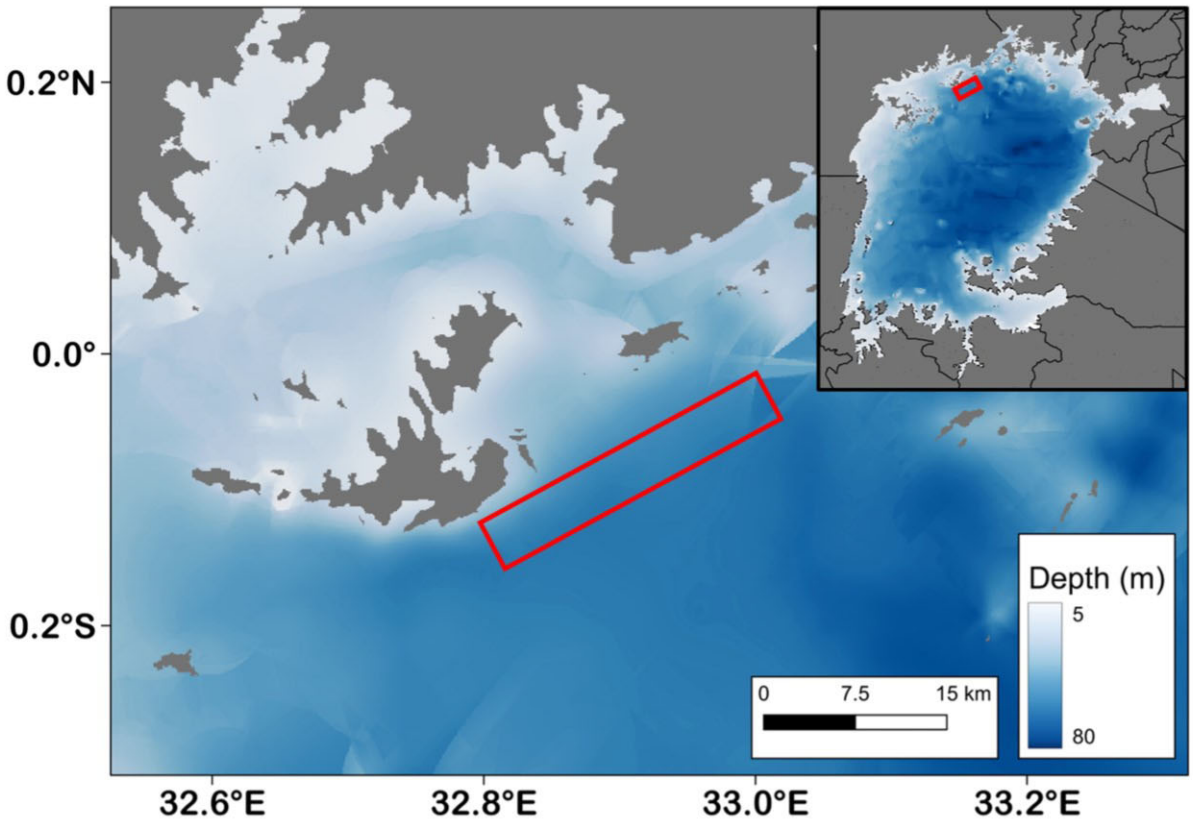

Figure 2. Map showing the acoustic and trawl net sampling areas in Lake Victoria, Uganda.

Table 1. Survey setting for the EK80 acoustic system, where FM is a frequency modulated pulse (chirp) and fast ramping mode indicates that the scattering amplitude is constant across the bandwidth (as opposed to slow ramping mode, where the amplitude of the lower and higher frequencies is reduced).

Setting	ES70-7C	ES120-7C	ES200-7C
Centre frequency (kHz)	70	120	200
Bandwidth (kHz)	45–90	90–170	160–250
Transmitting mode	FM	FM	FM
Power (W)	750	250	150
Sample interval (ms)	0.016	0.008	0.005
Pulse duration (ms)	1.024	1.024	1.024
Ramping mode	Fast	Fast	Fast
Ping interval (s)	1	1	1

were set to ping sequentially to mitigate the crosstalk between channels, but this was at the expense of a reduced probability of the same target/school being detected in all bands at the same time (Demer *et al.*, 2017). The Simrad EK80 system applies a Hann window to the transmitted pulse to taper the start and end of the pulse to suppress side lobes, which leads to a reduction in actual bandwidth (Demer *et al.*, 2017). In this study, 5 kHz were cut at each side of the band. All the 3 frequency bands were calibrated using a 38.1 mm diameter tungsten carbide sphere (peaks and nulls in the expected sphere TS by frequency were excluded from the calibration as indicated in Figure 3), following standard methods described by Demer *et al.* (2015). Calibration results showed that most of the band had an RMS (root mean square) error of <0.4 dB (Figure 3), which was deemed acceptable for further quantitative analysis.

Morphometric measurements by X-ray

We used a Fujifilm computed radiography X-ray radiograph suite (model CR-IR 392, detector plate dimensions of 35 × 43 cm) to obtain images of dagaa. The exposure factors were set to 50 kVp, 12 mAs, 2 s, and 0.95 m source-to-image distance (SID). In total, 115 fresh dagaa ranging in length from 2.5 to 6.1 cm were radiographed dorsally and laterally. Images revealed that most of the floating fish had distended swimbladders, that sinking fish had ruptured swimbladders, and that the swimming fish had what were apparently intact and naturally shaped (i.e. "normal" and undamaged) swimbladders. Figure 4 shows typical distended, intact, and ruptured swimbladders selected from floating, swimming, and sinking samples, respectively. Images from the 16 best-condition dagaa (that ranged in size between 2.8 and 5.4 cm) were selected to generate digitized files to define the shapes and dimensions of the dagaa body and gas-filled swimbladder for use in the subsequent modelling.

Scattering model

To model acoustic scattering from a single fish, the body and swimbladder were represented by a series of contiguous 1 mm-long cylinders. The length, height, and width (corresponding to the length and major and minor radii) of each cylindrical unit were measured from the X-ray images (.jpg files) using

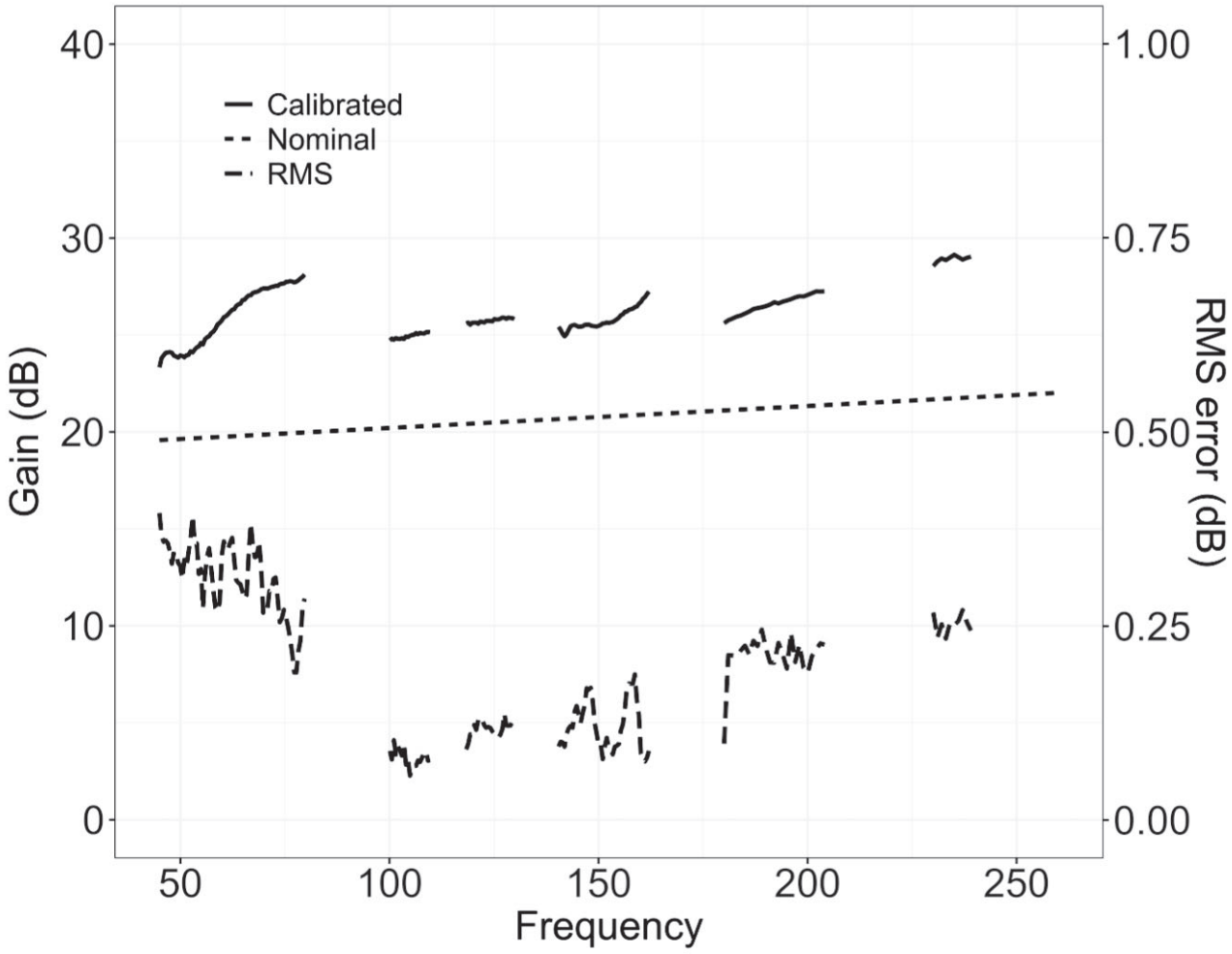

Figure 3. Calibration result of the broadband EK80 system, with RMS error (dashed line) generally <0.4. The dotted line and solid line indicate the nominal and calibrated gains of the system, respectively. The truncated frequency bands are dips of the theoretical TS of the 38.1 mm tungsten carbide calibration sphere.

Tps software (Rohlf, 2008, 2010). To reduce the bias while digitizing the outline of the fish and swimbladder, a three-point triangular average was used to smooth the shape (Horne *et al.*, 2000) (Figure 5). The measured morphometric parameters of the bodies and swimbladders were then used in the KRM model to simulate the acoustic backscattering from dagaa. Scattering from the body, anterior swimbladder, and posterior swimbladder were determined separately and combined coherently *a posteriori* (Li *et al.*, 2023).

The swimbladder and fish body volumes were estimated for each of the 16 fish by splitting the swimbladders and fish bodies into contiguous elliptic cylinders and summing the volumes of each unit to explore fish-to-fish variability. The total volume can be given by:

$$Volume = \sum_{1}^{N_s-1} \pi a_j b_j L_j \quad (2)$$

Where L_j is the jth cylinder along the fish vertebral column, and a and b are the radii of the major and minor axes, respectively, of each elliptic cylinder.

The KRM model assumes that for each cylindrical element with $ka > 0.15$ [where a is the minor radius of a cylinder element (m) and k is the wavenumber $= f\frac{2\pi}{c}$ with c = sound speed (m/s) and f = frequency (Hz)], backscatter from it can be approximated as an evaluation of the Helmholtz–Kirchhoff integral based on the projection of the cross-sectional area (σ_{bs}, m^2) of the cylindrical element on a plane normal to the incident wavefront. The transmission of the incident wave (ray path) between the fish body and swimbladder was constructed as in Clay and Horne (1992). The interference between the anterior and posterior swimbladders is not considered in the KRM model. Details of the KRM model can be found in Clay and Horne. (1992, 1994). The parameters for modelling were taken from another dual-chamber cyprinid species (*Mirogrex terraesanctae*) as reported in Horne *et al.* (2000), in which the sound speeds through the swimbladder, fish body, and water were 345, 1575, and 1485 m/s, respectively, and the densities of the swimbladder, fish body, and water were 2.64, 1080, and 1000 kg/m^3, respectively. The incident angle (θ) was modelled over the range 65–115° as described above, where $\theta > 90°$ is head up, 90° is normal to the vertebral column, and $\theta > 90°$ is head down.

To quantify variation in backscattering amplitude across a range of dagaa sizes and morphologies, mean and standard deviations of backscattering intensity across all 16 fish were computed as a function of fish length, tilt, and acoustic wavelength. To make the echo amplitudes from all 16

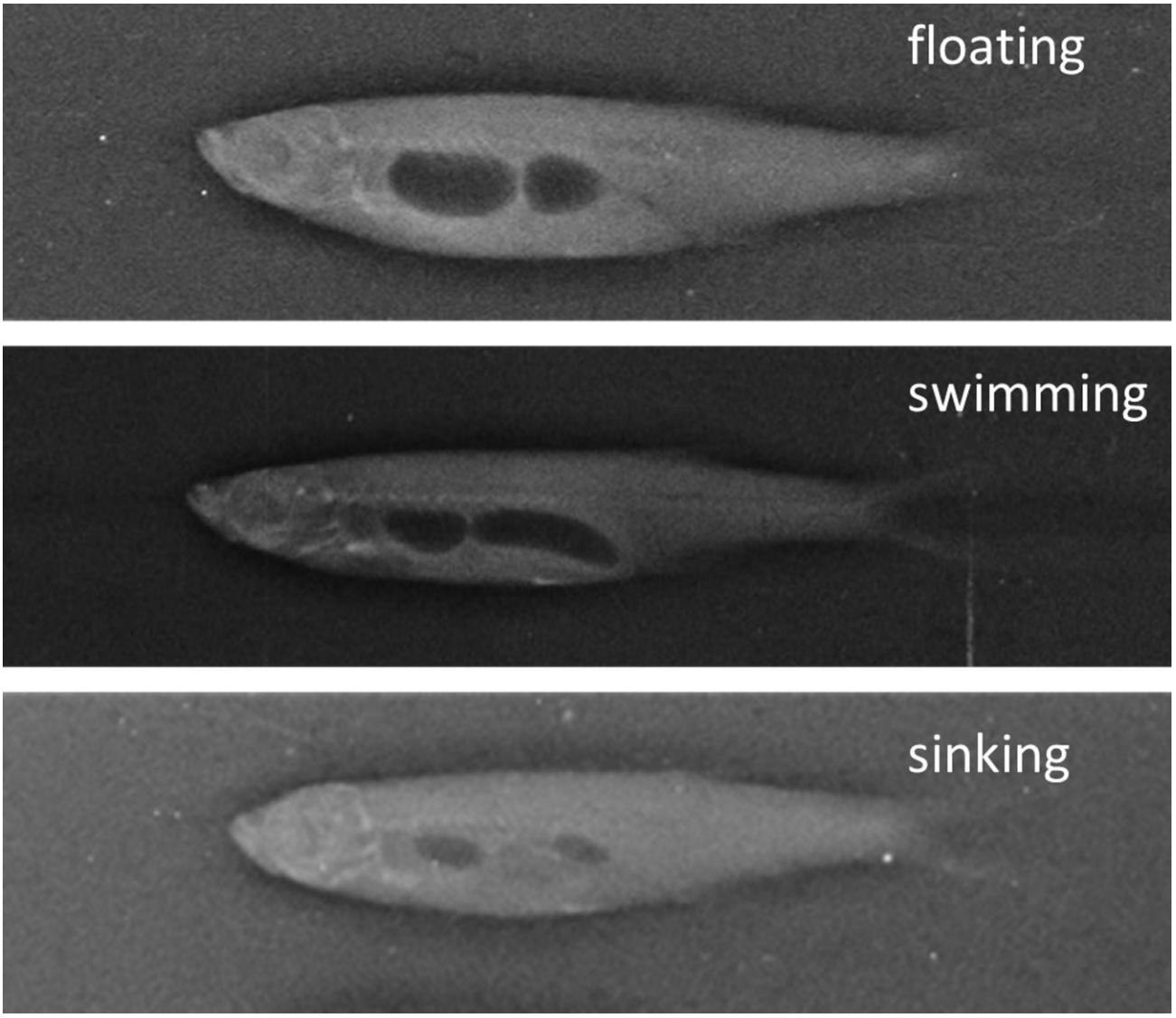

Figure 4. Lateral view of X-rayed dagaa from floating, swimming, and sinking dagaa, which shows a distended (top), natural (middle), and ruptured (bottom) swimbladder, respectively.

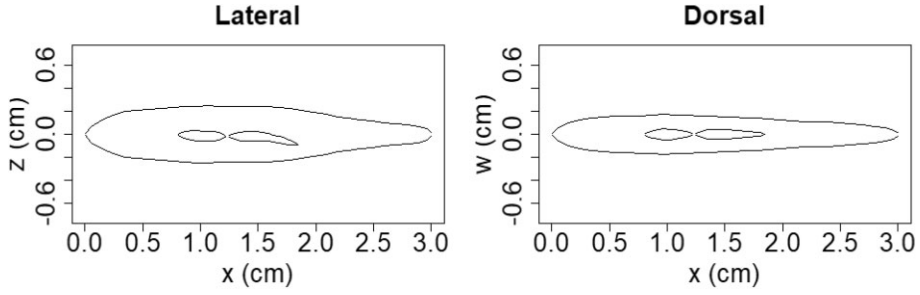

Figure 5. Lateral and dorsal outline of the X-ray morphometric measurements of a dagaa with a standard length (SL) of 3.0 cm.

X-rayed samples directly comparable, they were all modelled at a SL of 4 cm. If the tilt angle of an object is held constant, the backscattering amplitude is mainly a function of the size of the object relative to the wavelength [L/λ, where L is the length and λ is the wavelength ($\frac{c}{f}$)]. By scaling all 16 fish to a SL of 4 cm, L/λ will only show the effect of changes in acoustic frequency (i.e. 45–250 kHz) on echo amplitude. The scattering amplitude was inspected as a linear unitless reduced scattering length (RSL) as a function of L/λ and tilt, which is given by:

$$RSL = L_{bs}/L \tag{3}$$

In order to compare the KRM model predictions [$TS(f)$] to the *in-situ* measured volume backscattering strength ($S_v(f)$),

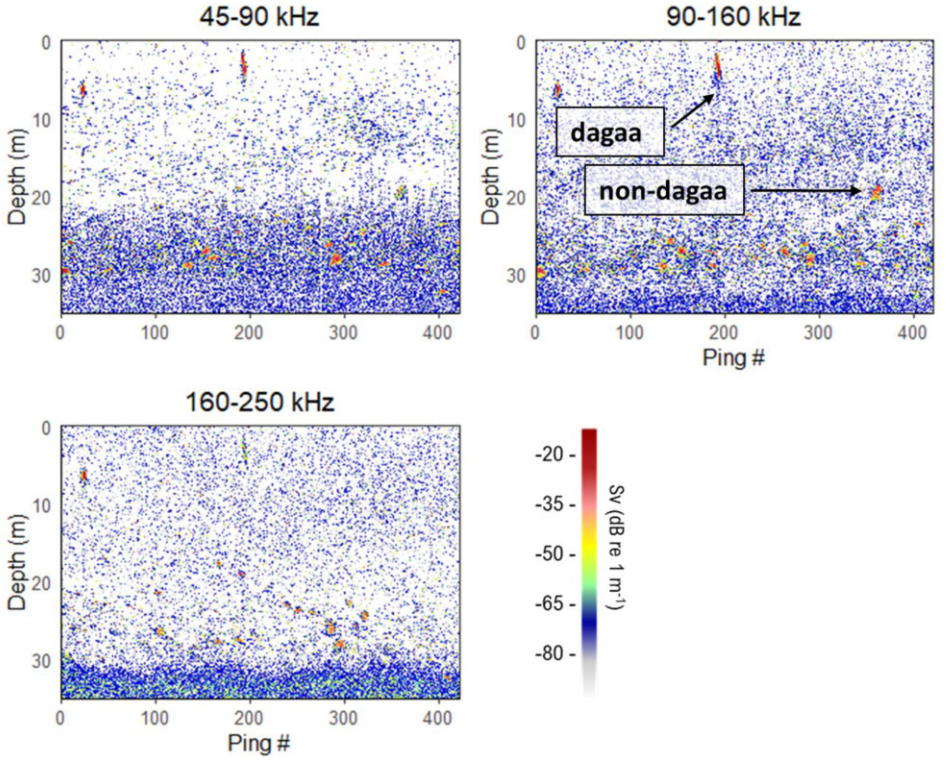

Figure 6. A typical series of pulse-compressed echograms over the 3 frequency bands showing the "needle-like" feature of dagaa school.

dagaa schools were isolated in the echograms by visually identifying their needle-like appearance on the pulse-compressed echogram (Figure 6, upper right panel). Further, the *in-situ* data were only processed if dagaa dominated in the trawl catch by mass (>99%). The $S_v(f)$ of each dagaa school was exported by applying a fast Fourier transform (FFT) window of length 0.4 m to the pulse-compressed echogram, following the recommendation by Benoit-Bird and Waluk (2020). Backscattering by a school of dagaa represents the summation of backscattering by all individual fish in the school; hence, we simulated backscattering for individual fish [i.e. KRM predicted $TS(f)$] and scaled it up by different densities to generate school backscattering (i.e. we conducted forward prediction). School backscattering will, of course, be dependent on the sizes and tilts of the fish in the school. For the forward prediction, length distributions of dagaa were taken into account by weighting the cross-sectional area (length-weighted σ_{bs}) by the proportion of the length class (by a 1 mm interval) in the length distribution from the trawl (Jech *et al.*, 2017). Tilt-angle distribution was determined by a tracking method as described below. Due to a lack of information on the packing density of fish in schools, a relative school scattering response $[r(f)]$ (Korneliussen and Ona, 2003), which removes the effect of packing density, was introduced:

$$S_V = 10log10\,(\sigma_{bs}) + 10log10\,(\rho) = TS + 10log10\,(\rho) \quad (4)$$

$$r\,(f) = Sv_i - S_{V70} = TS_i - TS_{70} \quad (5)$$

where ρ is the actual fish density in a school and thus can be removed, and S_V is the summation of individual fish scattering in the linear domain. The mean and confidence intervals (95%) of $r(f)$ for *in-situ* measured schools over a wide bandwidth were generated by using a reference frequency (70 kHz). The mean and confidence intervals (95%) of $r(f)$ for the KRM prediction were computed from the variability across the 16 intact X-rayed fish, using the same reference frequency. The model prediction $[TS(f)]$ for each individual fish of the 16 was scaled up by a series of fish densities (from 1 to 100 ind./m^3, in steps of 0.1) to visualize the similarity of the spectra between the KRM predictions and *in-situ* measurements.

Tilt-averaged TS–TL relationship

The RSLs arising from the KRM models of the 16 X-rayed fish were used to derive a tilt-averaged TS_θ to TL relationship by fitting a linear least squares regression. TS_θ was calculated by randomly sampling 5000 tilt angles from a normal distribution defined by parameters from the *in-situ* tracking method (Equation 6), and the KRM predictions for those tilts for all 16 fish were then averaged in the linear domain. The normal distribution of the dagaa tilt angles was determined from the *in-situ* measured tracks of single fish in regions where dagaa dominated by mass (>99%) in the trawl catch. Single targets were detected using the single echo detection (SED) and tracking module (Blackman, 1986) in Echoview 12.1 (Echoview Software Pty Ltd, 2021), with the following settings: minimum threshold -65 dB at 120 kHz; pulse length determination level (PLDL) 6 dB; minimum and maximum normalized pulse lengths 0.4 and 1.5, respectively; beam compensation 6 dB; and maximum standard deviations of major and minor axes 3°. Tracks were only accepted as targets if at least three consecutive pings met the selection criteria. Tracking is based on the 3D displacement of a single fish as follows:

$$tilt = \arcsin\left(\frac{z^2}{\sqrt{x^2+y^2+z^2}}\right) \quad (6)$$

Table 2. Modelled 16 dagaa reporting their SL, TL, M, the volume of the fish body (V_{fb}), anterior swimbladder (V_{asb}), and *posterior* swimbladder (V_{psb}), and proportion of the swimbladder to the fish body.

SL (cm)	TL (cm)	M (g)	V_{fb} (cm^3)	V_{asb} (cm^3)	V_{psb} (cm^3)	Proportion %
2.7	3.2	0.4	0.24	0.003	0.004	2.7
4.0	4.7	1.1	0.72	0.012	0.008	2.7
2.4	2.8	0.3	0.12	0.002	0.002	3.0
3.0	3.5	0.5	0.23	0.004	0.006	4.5
2.6	3.0	0.4	0.13	0.003	0.004	5.8
4.5	5.2	1.4	0.79	0.005	0.015	2.6
4.0	4.7	1.1	0.81	0.012	0.024	4.5
3.5	4.1	0.8	0.37	0.005	0.018	6.3
3.5	4.1	0.8	0.41	0.004	0.017	5.2
4.3	5.0	1.3	0.62	0.008	0.027	5.5
4.0	4.6	1.0	0.59	0.012	0.021	5.6
4.2	4.9	1.2	0.61	0.010	0.025	5.6
4.5	5.2	1.4	0.87	0.024	0.048	8.2
3.6	4.2	0.8	0.45	0.008	0.016	5.1
4.3	5.0	1.3	0.90	0.013	0.040	5.9
4.6	5.4	1.5	1.06	0.018	0.051	6.5

where x and y are the fish movement distance alongship and athwartship, and z is the depth/vertical displacement. The tilt of fish in tracks ranged from 90 to -90°, where 0° indicates a horizontal orientation, positive is head up, and negative is head down. The tilt inference only considers the position of the first and last detections in the track and assumes that these 2 points are connected by a straight line, so tracks with a tortuosity >1.3 (i.e. convoluted tracks where orientation may change within the track) were excluded from further analysis (Henderson *et al.*, 2008). More details on single-target tracking can be found in Blackman (1986). The resulting tilt angle distribution was input to the KRM model approximation to enable a fit of the tilt-averaged TS–TL relationship by linear regression as follows:

$$TS_\theta = a log10 + b_a \quad (7)$$

$$TS_\theta = 20 log10 + b_{20} \quad (8)$$

where a is the unknown slope, and b_a and b_{20} are the intercepts of the regressions. TS–TL relationships were modelled at 70, 120, and 200 kHz (the frequencies used most commonly during acoustic surveys in Lake Victoria). All the regressions, model predictions, and calculations were performed in R 4.0.1 (R Core Team, 2021). The KRM simulations were performed using the R package KRMr (Gastauer, 2023).

Results

Intra-specific variability

A total of 115 dagaa were measured by X-ray, of which we identified 16 as having sufficiently intact morphological conditions for the construction of scattering models. The TL of the dagaa used for modelling ranged from 2.8 to 5.4 cm ($n = 16$, with a mean of 4.35 ± 0.83 s.d.), and their masses ranged from 0.3 to 1.5 g (Table 2). The volume of the fish, excluding the caudal fin, ranged from 0.12 to 1.13 cm^3, with the swimbladder accounting for between 2.6 and 8.2% of the total volume of each fish (Supplementary Figure S1a). The average proportion of the swimbladder volume to the total fish body volume was 4.9%. TL of fish was positively and significantly correlated with the volume of the fish body ($r = 0.94$, $n = 16$, $p < 0.001$) (Supplementary Figure S1a) and with the volumes of both the anterior ($r = 0.74$, $n = 16$, $p < 0.01$) and posterior swimbladders ($r = 0.79$, $n = 16$, $p < 0.001$) (Supplementary Figure S1b and S1c). The relationship between fish TL and the proportions of backscattering from the swimbladder and fish body revealed a negative trend with size, but the correlation was not significant at a level of 5% ($r = -0.06$, $n = 16$, $p = 0.81$) (Supplementary Figure S1d). The relationship between the total swimbladder volume (V_{sb}) and fish TL indicated negative allometric growth of the swimbladder ($V_{sb} = 0.0046TL^{3.21}$, $R^2 = 0.92$), where the slope of 3.21 is the allometric coefficient (AC). An AC of 1 represents isometry, while AC >1 is negative allometry (Yasuma *et al.*, 2010). This means that, in dagaa, the body volume grows more rapidly than the swimbladder volume. According to the predicted masses of the 16 X-rayed fish (weighing was not accurate for the frozen fish samples), all fish had a body volume (without swimbladder, in cm^3) less than their body mass (in gramme), thus giving a density >1 g/cm^3, which implies that extra buoyancy may be needed from the swimbladder or oily tissue if the fish are not to have to swim continuously to maintain horizontal position in the water column.

Scattering variability

KRM model simulations of the backscattering from the swimbladder and body were made separately for each of the 16 selected dagaa. The results showed that the swimbladder accounted for between 65% and 90% of scattering (of whole fish) at a dorsal incident angle at 120 kHz. The linear mean and standard deviation of the RSL of the 16 modelled dagaa, as a function of tilt angle and L/λ, are shown in Figure 7. Over the range of tilt angle from 65 to 115°, and L/λ range from 1 to 7, the mean RSL varied from 0.01 to 0.08. When the L/λ is <4 (corresponding to a frequency of ca. 150 kHz in this case), the RSL peaked at around a tilt angle of 90° and reduced symmetrically as the tilt angle deviated positively or negatively (i.e. head up or head down) from the dorsal aspect. Less directivity was apparent at low frequencies, whereas at high frequencies (>150 kHz), more directivity was apparent (i.e. RSL was more influenced by the tilt angle). The deviation of the RSL indicates that the RSL changes the most when the tilt angle is close to the dorsal incident angle.

An individual dagaa with an SL of 3.5 cm was selected from the 16 dagaa samples to model the variation of TS at various

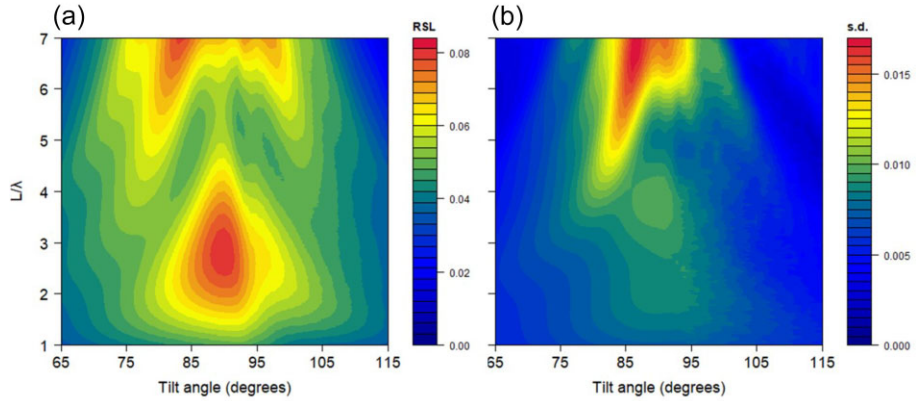

Figure 7. The mean (a) and standard deviation (b) of RSL for 16 modelled dagaa as a function of L/λ and tilt angle (°), where the tilt = 90° represents broadside incidence, tilt >90° indicates heads up and tilt <90° is heads down. All samples were scaled to a SL of 4 cm.

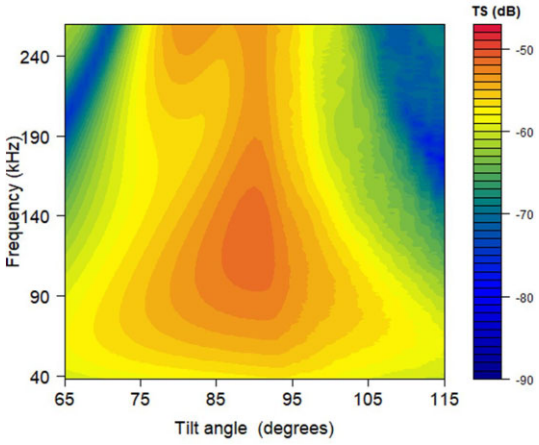

Figure 8. Simulated TS of a dagaa as a function of frequency (40–250 kHz) and tilt angle (65–115°, where 90° represents broadside incidence) for a dagaa with a SL of 3.5 cm.

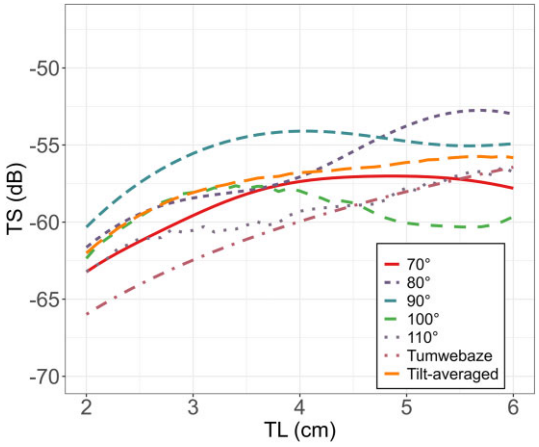

Figure 9. Simulated mean dagaa TS at 120 kHz from 16 X-rayed dagaa at different tilt angles as a function of length. The tilt-averaged TS was derived from a tilt distribution (100 samples) with a mean of 93.5° and s.d. of 15.1°, spanning from 65 to 115° at 1° intervals (orange line). The TS–TL relationship developed by Tumwebaze (2003) is shown for comparison with the model simulations (dashed purple line).

frequencies and tilt angles (see Figure 8): this individual was chosen because it had a size closest to the mean of all fish samples and possessed a well-preserved swimbladder. At frequencies <170 kHz, the maximum backscattering intensity from the single chosen dagaa occurred at a tilt angle of about 90° (dorsal-aspect incidence). At frequencies <70 kHz, backscatter from the chosen dagaa was not sensitive to changes in tilt angle. As the frequency increased, at L/λ ≈ 4, the scattering strength began to become more sensitive to the change in tilt angle. The predicted TS was highly dependent on tilt angle, varying by 14.0 dB at 120 kHz across the tilt range 65–115° (where 0° is head up and 180° is tail up), and TS variability with tilt generally increased with increasing frequency. At an angle of about 80°, when the dagaa was in a head-down posture, the scattering is more complex than for the horizontal and head-up postures, which is a consequence of the tilt angle of the posterior swimbladder. As the frequency increased, a non-monotonic increase of TS was observed; for example, at a fixed tilt angle of 90°, the TS peaked at around 90 kHz and decreased as the frequency increased.

KRM-modelled TS was compared to the TS–TL relationship developed by Tumwebaze *et al.* (2003), which is the relationship used presently to determine dagaa biomass from lake-wide acoustic survey data. Figure 9 depicts the estimation of TS from Tumwebaze *et al.* (2003) for dagaa as a function of TL, as well as the estimation of mean TS from the KRM model for the 16 modelled dagaa at a set of different tilt angles (70, 80, 90, 100, and 110 degrees). At a tilt angle covering the majority of the KRM model simulation range (70–110°), the KRM model TS predictions were generally higher than those from the traditional empirical formula, with a maximum difference in TS of 7 dB for fish with body lengths in the range from 2 to 6 cm. KRM model simulations and predictions from the Tumwebaze *et al.* (2003) TS–TL relationship are closest at a tilt angle of 110°.

Comparison of model prediction and *in-situ* measurements

A total of 92 dagaa schools were selected from the trawling region where dagaa dominated the catch by mass (>99%) to derive *in-situ* measured backscattering spectra to compare with the length-weighted KRM model predictions presented in Figure 10. The amplitude of the mean KRM model predicted $S_V(f)$ could be made to match with the *in-situ* measurements when the school packing density was set to 18.2 ind./m^3

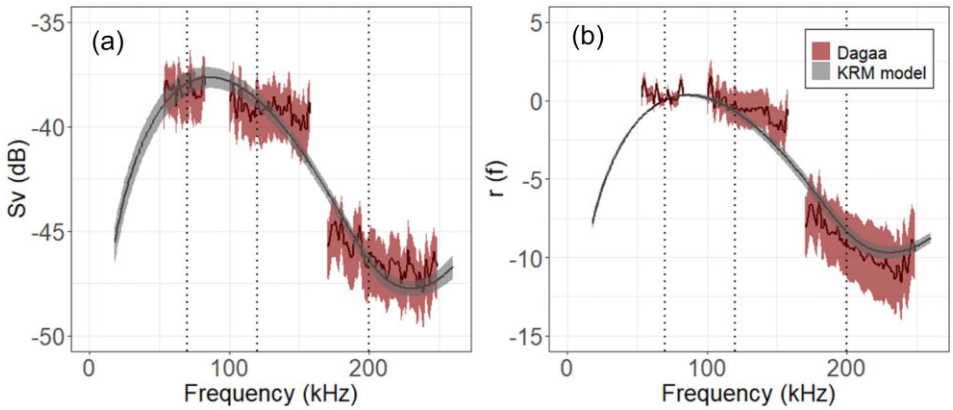

Figure 10. Comparison of in-situ measured and model predictions of Sv of dagaa schools (a), where the solid line is the mean Sv and the shaded area is the 95% confidence intervals of the Sv. The model prediction of schooling dagaa was scaled to a density of 18 ind./m^3 to match the *in-situ* measurements. The right panel (b) is the relative frequency response of *in-situ* measured schools and model predictions. In total, 92 schools were empirically selected from the trawling area by their "needle-like" features. Dotted lines indicating the nominal frequency, 70, 120, and 200 kHz, for the transducers used in this study.

(Figure 10a). The $r(f)$ of the *in-situ* measured schools varied between -11.6 and 1.6, whereas the KRM model predictions ranged from -9.7 to 0.3 (Figure 10b). The amplitudes of the $r(f)$ agreed well between the *in-situ* measurements and the model predictions. Generally, the $S_V(f)$ of dagaa peaked at the lower end of the frequency spectrum, between 50 and 100 kHz (the transit region between Rayleigh and geometric scattering, where the wavelength starts to become smaller than the size of the scatters), and decreased from 100 kHz onwards. The discrepancies between the mean $r(f)$ *in-situ* measurements and the KRM model predictions ranged from -2.9 to 3.1 dB at all frequencies, with variation across the spectrum (the largest discrepancy was at 157 kHz). The variability in the measured (school-to-school) relative frequency response increased with frequency non-monotonically, which was also the case in the model predictions (Figure 10).

Tilt-averaged TS–TL relationship

In total, 993 individual dagaa tracks with >3 acceptable pings and low tortuosity were identified. Tilt angles inferred from them were used to generate a Gaussian distribution of tilt: the distribution had a mean and s.d. of 93.5 and 15.1°. To enable transformation between TL to SL (TL–SL) for modelling (caudal fin length was not included in the model), 200 individual dagaa were measured, and a TL–SL relationship was derived ($TL = 1.156 \times SL + 0.0523$; $r^2 > 0.99$, $n = 200$). The TS–TL relationships from regression analysis from the 16 KRM model predictions, with a slope of a and fixed slope 20 (Equatuions 7 and 8), at 3 commonly used acoustic-survey frequencies (70, 120, and 200 kHz) are listed in Table 3. The regressions that were constructed with a slope that was permitted to vary had residual standard errors (s.e.) ranging from 0.21 to 0.32, and the error increased with frequency, while the regressions with a standard fixed slope of 20 showed higher residual s.e., with a range of 1.95–2.85 (Table 3). Regressions with an intercept of b_a had a lower slope than the standard slope of 20 at 70 and 120 kHz, resulting in lower TS for large fish and higher TS for small fish as compared to the standard slope regression. The regression at 120 kHz with a slope of -19.49 and an intercept of -70.29 results in a TS that is 1.5 dB higher than the traditional standard TS–TL relationship [$TS_{120\ kHz} = 20\log(TL) - 72.2$].

Table 3. Linear regression fitted tilt-averaged TS to fish TL relationship for the most commonly used frequencies in the Lake Victoria survey, based on KRM prediction.

f (kHz)	$TS_\theta = a\log_{10}(TL) + b_a$			$TS_\theta = 20\log_{10}(TL) + b_{20}$	
	Slope (a)	b_a	s.e.	b_{20}	s.e.
70	17.16	−66.80	0.21	−68.63	1.95
120	19.49	−70.29	0.23	−70.63	2.25
200	26.83	−74.25	0.32	−69.84	2.85

The slopes (a), intercepts (b_a and b_{20}) and the residual s.e. of the regression corresponding to each frequency are reported.

Discussion

This study used a KRM model to predict the broadband scattering properties of dagaa and to derive tilt-averaged TS–TL relationships at the acoustic frequencies used most commonly for fisheries surveys in Lake Victoria (i.e. 70, 120, and 200 kHz). At present, dagaa biomass estimates are based solely on 120 kHz data (due in part to a lack of TS information at 70 and 200 kHz). Model predictions of TS made here across a range of frequencies will enable a valuable archive of historic survey data collected at 70 and 200 kHz to be reprocessed and hence to deliver an updated time series of dagaa biomass. Furthermore, this study is the first application of broadband acoustics in Lake Victoria. Good agreements between model simulations and *in situ* observations were found. The results of this study demonstrate the potential of using broadband acoustics for species classification and hence pave the way for further developments in this area towards improved multi-species biomass estimates, which is in line with the LVFO's aspiration to move towards EBFM of Lake Vicotria.

Intra-specific variability

Our analyses reveal that the swimbladder of dagaa is the main acoustic scattering source at 120 kHz, accounting for between 65 and 90% of the total backscattering intensity. The relationship between TL body and swimbladder volume was positive, suggesting negative allometric growth of the swimbladder. The relationship between dagaa body length and the proportion of backscatter from the swimbladder was not statistically significant, but suggests that larger fish typically elicit a

lower proportion of backscatter from their swimbladder than do smaller fish. The KRM-modelled intra-specific acoustic backscattering amplitude variation we detected in dagaa can either be attributed to sampling bias (e.g. body/swimbladder shape distortion) or to anatomical and/or physiological differences. In the observations of Clay and Horne (1992), older fish showed a larger swimbladder tilt than younger fish, and the swimbladder volumes. The densities of fish bodies also vary seasonally and regionally (Lloret-Lloret *et al.*, 2020). Such changes in tilt angle, body fat, and bone content will in turn influence backscattering from the fish. According to Davenport (1999), the swimbladders of freshwater fish (*Salmo salar, S. trutta*, and *Gymnocephalus cernuus*) account for no >7% of the total body volume, but here our measurements showed that the swimbladder of dagaa accounted for between 2.6 and 8.2% of the total body volume, with a mean value of 4.9%. The estimated body density, based on the volume and the M of dagaa samples, resulted in a fish density of <1 g/cm^3, which might indicate that extra buoyancy is needed for dagaa to maintain a vertical position in the water column without active swimming (which is energetically costly). The fish body density used in the KRM model (taken from Horne *et al.*, 2000, because that study was on a fish with a dual-chambered swimbladder) was 1.08 g/cm^3, which is higher than the estimated density from the modelled dagaa volume and mass. The modelled dagaa density may be in error as the accuracy of the volume estimate is dependent on the number of cylinders used to represent the body and the estimated mass is dependent on the emperical length-mass relationship. The empirical length-mass relationship of dagaa can be influenced by their body-fat content and other factors that can vary seasonally but were not verified in this experiment. A comprehensive length–M relationship (e.g. that takes seasonality into account) or a standard body mass weighing approach (recalling that due to the small mass of dagaa, onboard weighing, even with motion-compensated scales is inaccurate) is necessary to further improve such comparisons as well as the stock assessment.

TS–TL relationship

The new tilt-averaged TS–TL relationship [$TS_{120\ kHz} = 19.49\log(TL) - 70.29$] based on the KRM approximation resulted in an increase in TS compared to the relationship presently used [$TS_{120\ kHz} = 20\log(TL) - 72.2$] (Tumwebaze *et al.*, 2003). Adoption of the new relationship would lead to a substantial reduction in absolute biomass estimates. For example, with the difference of the intercept of 1.5 dB, a dagaa school containing fish with a mean length of 5.3 cm (resulting in a mean dagaa target strength per kg of -27.8 dB/kg) will see a reduction in its estimated biomass by 30%.

The LVFO and international partners have been conducting annual or biennial acoustic surveys on Lake Victoria for the past two decades, but there have been few opportunities so far to explore the acoustic scattering properties of dagaa by modelling. The standard TS–TL relationship [$TS_{120\ kHz} = 20\log(TL) - 72.2$] used presently to determine dagaa biomass was developed by Tumwebaze (2003), who measured total backscatter from known numbers of dagaa in a cage (measurement of between 370 and 2379 fish) and regressed backscattering intensity against the average TL of fish in the cage and inferred TS. That *in-situ* experimental design faced several challenges, such as the high rate of mortality of dagaa during capture, handling, and the experimental process (the percentage of live dagaa across 4 sets of experiments ranged from 0.1 to 12.5%): reductions in the numbers of live fish through the experiment, in particular, could have had a major impact on inferred TS and on inferred TS-to-length since small dagaa had higher mortality than large fish during the acoustic recording. In addition, the tilt angle, a crucial factor in backscattering amplitude, was not considered in that experiment. The modelling approach used here has the advantage that the influence of size and tilt can be explored, but model output is dependent on the density (the estimated fish density is <1 g/cm^3, which needs to be further verified) and sound speed contrasts input, and we were not able to determine those here.

Tilt dependence of TS

The backscattering intensity of a given object varies as a function of the size of the object with respect to the wavelength ($\lambda = \frac{c}{f}$, where c is the sound speed and f is the frequency). A change in tilt angle will influence the cross-sectional area [$\sigma_{bs} = 10^{(\frac{TS}{10})}$] and therefore TS. Our simulation of backscattering from a dagaa with 3.5 cm SL showed that changes in tilt angle led to variations in TS at 120 kHz of up to 14.0 dB, which would equate to a change in inferred biomass by a factor of 25. The KRM model simulation showed that backscatter intensity is more tilt-sensitive at higher frequencies (especially higher than 150 kHz) than at lower frequencies. Dagaa are an obligate schooling fish; for many fish species, schools are comprised of similarly sized fish, and fish in schools have polarized swimming angles (Partridge, 1981; Ranta *et al.*, 1992). The tilt angle distribution [93.5, 15.1] estimated by tracking single fish in the trawling area where dagaa dominated the catch by mass (>99%) is in general agreement with observations of tilt-angle distributions reported by Foote *et al.* (1987) for a variety of teleosts. They found that fish are typically tilted between 4° head down and 12° head up. The swimming angle of fish can vary with their behaviour, for example, if they are feeding, avoiding predators, or undertaking diel vertical migration. Huse and Ona (1996) and Tanoue *et al.* (2013) both describe a fish tilt angle distribution as arising from a "rise and glide" swimming strategy, which indicates a bimodal distribution of fish tilt during the day and night. Since DVM has been observed in dagaa (Goudswaard *et al.*, 2004), we may infer that there is also a diurnal effect in the tilt angle distribution of dagaa that will influence their acoustic backscattering amplitude and spectra. Acoustic surveys of fish in Lake Victoria are presently restricted to daylight hours (because of navigational and manning constraints), so biomass estimation is not likely to be muddied by DVM. Additionally, different tilt angle distributions can impact regression-based tilt-averaged TS–TL relationships. For example, Fässler *et al.* (2013) found that by simulating a wider dispersion of the tilt distribution (increasing s.d. from 5 to 20°) of boarfish (*Capros aper*), the intercept of a regression with a standard fixed slope of 20 was reduced by 1.5 dB. Henderson *et al.* (2007) also reported that, for Pacific hake (*M. productus*), using tilt-averaged TS and dorsal-aspect-only TS varied the regression intercept by 10 dB at a fixed slope of 20. The standard acoustic survey for dagaa only occurs in the daytime. If practical limitations on daylight-only operations for acoustic surveys on Lake Victoria are removed, further observations of tilt variation will be needed to enable compensation for light-driven variability in behaviour and hence TS.

Depth dependence of TS

Dagaa, as physostomes, do not possess a gas gland to inflate the swimbladder. Therefore, the swimbladder volume of dagaa will decrease when they move into deeper water, according to Boyle's law. Their TS might decrease as a result of the swimbladder compressing. The cross-section at z m depth can be described as:$\sigma_z = \sigma_0(1 + \frac{z}{10})^{\gamma}$, where σ_0 is the cross-section (m^2) at the surface, z is depth (m), γ is the contraction rate, which, for a free balloon, has a value of -0.67. Assuming the dagaa swimbladder follows a contraction rate of -0.23, as estimated by Ona (2003) for herring (*C. harengus*), the TS at 20 m depth will be 0.4 dB less than at 10 m depth. This depth-related change could be included in the TS–TL relationship as: $TS = 20\log(TL) + b_{20} - 10\log(1 + z/10^{\gamma})$. For dagaa, a decrease in mean TS with increases in depth has been observed by Tumwebaze (2003) but not quantified. The compression of the swimbladder is not necessarily isotropic. For example, the swimbladder of herring has a larger contraction rate in the lateral dimension than in the dorsal dimension, which means different contraction rates at the dorsal and lateral dimensions should both be considered (Fassler, 2010). The dual-chambered structure of the dagaa swimbladder adds another possible layer of complexity, and there is a lack of knowledge on the interaction in terms of volume change between the anterior and posterior sections. Smith and Croll (2011) have reported that the posterior chamber of cyprinid fish tends to be more extendable. When the fish is stimulated under norepinephrine exposure, the posterior chamber extends without changes in volume, while the anterior chamber is more likely to have a reduced volume. Lake Victoria is generally shallow (mean depth of 40 m), but nevertheless in pursuit of accurate biomass estimation, the potential for dagaa TS to vary with depth ought to be borne in mind.

Potential for species identification

The *in-situ* measured dagaa school scattering matched well with the KRM model predictions. This suggests that broadband data could be useful for school-level identification of dagaa. Assuming that the backscattering from the fish school is a linear superimposition of the cross-sectional area of individual fish within it (the principle of linearity that underpins echo integration), the KRM-model-predicted school backscattering will be a function of tilt angle, length of fish, and school density. In this study, variation in tilt angle brought more variation to the school scattering than fish length distribution. The tilt angle distribution can impact the amplitude of school backscattering considerably (14.0 dB at 120 kHz across the tilt range 65–115°, Figure 8) and, even more so, the characteristics of the spectra, whereas the length distribution primarily influences the amplitude (Figure 7a). Fish packing density is another vital factor in determining the amplitude of the school backscattering, but on the occasions where relative frequency responses are applied, the density can be disregarded. Given the increasing variation and sensitivity in school scattering with frequency, it may be beneficial to include a lower frequency (<150 kHz) in a species-identification method to enable discrimination between dagaa and other species (that in Lake Victoria include haplochromine cichlids, tilapia, and the crustacean *Caradina*) at the school/aggregation-level.

Suggestions for future work

Even though some matters such as the potential acoustic interference between scattering from the swimbladders, the swimbladder contraction mechanism, and the behaviour of dagaa were not explicitly addressed in this study, the KRM modelling method and comparison with broadband observation data do open the way for the subsequent series of experiments on dagaa TS. In light of the above discussions, there are two aspects to start with to improve the dagaa stock assessment: (1) improve the species partitioning/identification method. This could be attained by employing the broadband spectra for multifrequency species identification (Brierley *et al.*, 1998) or the automated machine learning classification (Proud *et al.*, 2020); and (2) incorporating the model-informed TS data with environmental, seasonal, and regional variability to deliver a fine-scale TS–M conversion factor and biomass reappraisal.

Acknowledgements

We are grateful to the Masters, crew and scientists from the Lake Victoria Fisheries Organization (LVFO), the National Fisheries Resources Research Institute (NaFIRRI, Uganda), the Tanzania Fisheries Research Institute (TAFIRI), and the Kenya Marine and Fisheries Research Institute (KMFRI) for their assistance with project coordination and participation in fieldwork.

Supplementary data

Supplementary material is available at the *ICESJMS* online version of the manuscript.

Conflict of interest

The authors declare no conflict of interest.

Funding

YY was funded by the China Scholarship Council. This work was supported by a grant from the UK Royal Society under the "International Collaboration" theme to ASB and RJK.

Data availability

The data underlying this article will be shared on reasonable request to the corresponding author.

References

Antona, A. 2016. Remote Fish Species and Size Identification Using Broadband Echosounders. Institute for Marine Resources and Ecosystem Studies (IMARES), Wageningen University. 1–84.

Benoit-Bird, K. J., and Waluk, C. M. 2020. Exploring the promise of broadband fisheries echosounders for species discrimination with quantitative assessment of data processing effects. The Journal of the Acoustical Society of America, 147: 411–427.

Blackman, S. S. 1986. Multitarget Tracking with Radar Applications. Artech House, Inc., Dedham, MA. 232.

Brierley, A. S., Ward, P., Watkins, J. L., and Goss, C. 1998. Acoustic discrimination of Southern Ocean zooplankton. Deep Sea Research Part II: Topical Studies in Oceanography, 45: 1155–1173.

Clay, C. S., and Home, J. K. 1994. Acoustic models of fish: the Atlantic cod (*Gadus morhua*). The Journal of the Acoustical Society of America, 96: 1661–1668.

Clay, C. S., and Horne, J. K. 1992. Acoustic models and target strengths of the Atlantic cod (*Gadus morhua*). The Journal of the Acoustical Society of America, 92: 2350–2351.

Davenport, J. 1999. Swimbladder volume and body density in an armoured benthic fish, the streaked gurnard. Journal of Fish Biology, 55: 527–534.

Demer, D. A., Andersen, L. N., Basset, C., Berger, L., Chu, D., Condiotty, J., Cutter, G. R. *et al.*. 2017. Evaluation of a wideband echosounder for fisheries and marine ecosystem science. ICES Cooperative Research Report No. 336. 69.

Demer, D. A., Berger, L., Bernasconi, M., Bethke, E., Boswell, K., Chu, D., Domokos, R. *et al.* 2015. Calibration of acoustic instruments. ICES Cooperative Research Report No. 326. 133. https://doi.org/10.17895/ices.pub.5494

Demer, D. A., and Conti, S. G. 2005. New target-strength model indicates more krill in the Southern Ocean. ICES Journal of Marine Science, 62: 25–32.

Echoview Software Pty Ltd. 2021. commercial sofeware, Hobart, Tasmania, Australia.

Fassler, S. M. M. 2010. Target strength variability in Atlantic herring (*Clupea harengus*) and its effect on acoustic abundance estimates. Doctoral dissertation, University of St Andrews: 1–214.

Fässler, S. M. M., O'donnell, C., and Jech, J. M. 2013. Boarfish (*Capros aper*) target strength modelled from magnetic resonance imaging (MRI) scans of its swimbladder. ICES Journal of Marine Science, 70: 1451–1459.

Foote, K. G. 1980. Importance of the swimbladder in acoustic scattering by fish: a comparison of gadoid and mackerel target strengths. The Journal of the Acoustical Society of America, 67: 2084–2089.

Foote, K. G., Aglen, A., and Nakken, O. 1986. Measurement of fish target strength with a split beam echo sounder. The Journal of the Acoustical Society of America, 80: 612–621.

Foote, K. G., and Ona, E. 1987. Tilt angles of schooling penned saithe. ICES Journal of Marine Science, 43: 118–121.

Gastauer, S. 2023. KRMr: Kirchhoff Ray Mode Model for fisheries acoustics. https://github.com/SvenGastauer/KRMr (last accessed 22 May 2023).

Gastauer, S., Scoulding, B., Fässler, S. M. M., Benden, D. P. L. D., and Parsons, M. 2016. Target strength estimates of red emperor (*Lutjanus sebae*) with Bayesian parameter calibration. Aquatic Living Resources, 29: 301.

Gastauer, S., Scoulding, B., and Parsons, M. 2017. Estimates of variability of goldband snapper target strength and biomass in three fishing regions within the Northern Demersal Scalefish Fishery (Western Australia). Fisheries Research, 193: 250–262.

Goudswaard, K., Wanink, J. H., Witte, F., Katunzi, E. F. B., Berger, M. R., and Postma, D. J. 2004. Diel vertical migration of major fish-species in Lake Victoria. Hydrobiologia, 513: 141–152.

Henderson, M. J., and Horne, J. K. 2007. Comparison of in situ, ex situ, and backscatter model estimates of Pacific hake (*Merluccius productus*) target strength. Canadian Journal of Fisheries and Aquatic Sciences, 64: 1781–1794.

Henderson, M. J., Horne, J. K., and Towler, R. H. 2008. The influence of beam position and swimming direction on fish target strength. ICES Journal of Marine Science, 65: 226–237.

Horne, J. K., Walline, P. D., and Jech, J. M. 2000. Comparing acoustic model predictions to in situ backscatter measurements of fish with dual-chambered swimbladders. Journal of Fish Biology, 57: 1105–1121.

Huse, I., and Ona, E. 1996. Tilt angle distribution and swimming speed of overwintering Norwegian spring spawning herring. ICES Journal of Marine Science, 53: 863–873.

Jech, J. M., Horne, J. K., Chu, D., Demer, D. A., Francis, D. T. I., Gorska, N., Jones, B. *et al.* 2015. Comparisons among ten models of acoustic backscattering used in aquatic ecosystem research. The Journal of the Acoustical Society of America, 138: 3742–3764.

Jech, J. M., Lawson, G. L., and Lavery, A. C. 2017. Wideband (15-260 kHz) acoustic volume backscattering spectra of Northern krill (*Meganyctiphanes norvegica*) and butterfish (*Peprilus triacanthus*). ICES Journal of Marine Science, 74: 2249–2261.

Korneliussen, R. J. 2018. Acoustic target classification. ICES Cooperative Research Report No. 344. 104.

Korneliussen, R. J., and Ona, E. 2003. Synthetic echograms generated from the relative frequency response. ICES Journal of Marine Science, 60: 636–640.

Li, C., Chu, D., Horne, J., and Li, H. 2023. Comparison of coherent to incoherent kirchhoff-ray-mode (KRM) models in predicting backscatter by swim-bladder-bearing fish. Journal of Marine Science and Engineering, 11: 473.

Lloret-Lloret, E., Navarro, J., Giménez, J., López, N., Albo-Puigserver, M., Pennino, M. G., and Coll, M. 2020. The seasonal distribution of a highly commercial fish is related to ontogenetic changes in its feeding strategy. Frontiers in Marine Science, 7: 1068.

LVFO. 2012. Regional Status Report on Lake Victoria Bi-ennial Frame Surveys between 2000 and 2012. Jinja, Uganda, 63.

LVFO. 2016. State of lake victoria dagaa (*Rastrineobola argentea*): quantity, quality, value addition, utilization and trade in the East African region for improved nutrition, food security and income. Jinja, Uganda, 3–17.

LVFO. 2019. A report of the Lake Victoria hydro-acoustic survey. Hydro-acoustics Regional Working Group, Jinja, Uganda. 88.

Manik, H. M. 2016. Quantifying fish backscattering using SONAR instrument and Kirchhoff Ray Mode (KRM) Model. Journal of Physics Conference Series, 739(1): 012055.

McClatchie, S., Thorne, R. E., Grimes, P., and Hanchet, S. 2000. Ground truth and target identification for fisheries acoustics. Fisheries Research, 47: 173–191.

Ona,, E. (2003) An expanded target-strength relationship for herring. ICES Journal of Marine Science, 60(3): 493.

Partridge, B. L. 1981. Internal dynamics and the interrelations of fish in schools. Journal of Comparative Physiology, 144: 313–325.

Proud, R., Mangeni-Sande, R., Kayanda, R. J., Cox, M. J., Nyamweya, C., Ongore, C., Natugonza, V. *et al.*. 2020. Automated classification of schools of the silver cyprinid *Rastrineobola argentea* in Lake Victoria acoustic survey data using random forests. ICES Journal of Marine Science, 77: 1379–1390.

R Core Team. 2021. R: A Language and Environment for Statistical Computing. https://www.r-project.org (last accessed 10 May 2023).

Ranta, E., Lindström, K., and Peuhkuri, N. 1992. Size matters when three-spined sticklebacks go to school. Animal Behaviour, 43: 160–162.

Rohlf, F. J. 2008. TpsDig, ver. 2.11. Digitize landmarks and outlines. Department of Ecology and Evolution, State University of New York, Stony Brook, NY.

Rohlf, F. J. 2010. tpsDig. Department of Ecology and Evolution, State University of New York, Stony Brook, NY.

Smith, F. M., and Croll, R. P. 2011. Autonomic control of the swimbladder. Autonomic Neuroscience, 165: 140–148.

Stanton, T. K., Chu, D., Jech, J. M., and Irish, J. D. 2010. New broadband methods for resonance classification and high-resolution imagery of fish with swimbladders using a modified commercial broadband echosounder. ICES Journal of Marine Science, 67: 365–378.

Taabu-Munyaho, A., Nyamweya, C. S., Sitoki, L., Kayanda, R., Everson, I., and Marteinsdóttir, G. 2014. Spatial and temporal variation in the distribution and density of pelagic fish species in Lake Victoria. East Africa. Aquatic Ecosystem Health and Management, 17: 52–61.

Tanoue, H., Komatsu, T., Natheer, A., Mitani, I., Watanabe, S., Watanabe, Y., Hamano, A. *et al.* 2013. Measurement of diurnal body tilt angle distributions of threeline grunt Parapristipoma trilineatum

using micro-acceleration data loggers. Journal of Marine Science and Engineering, 1: 3–9.

Tumwebaze, R. 2003. Hydroacoustic abundance assessment and population characteristics of Rastrineobola argentea in Lake Victoria. PhD Thesis. University of Hull. 23–115.

Tumwebaze, R. 2018. The status of Lake Victoria Fisheries under limited access fishery. *In* Global Conference on Tenure and User Rights in Fisheries 2018 Achieving Sustainable Development Goals by 2030. 1–6.

Yasuma, H., Sawada, K., Takao, Y., Miyashita, K., and Aoki, I. 2010. Swimbladder condition and target strength of myctophid fish in the temperate zone of the Northwest Pacific. ICES Journal of Marine Science, 67: 135–144.

Handling editor: Olav Rune Godø

Received: 11 June 2023; **Revised:** 10 August 2023; **Accepted:** 14 August 2023